



The Method of Fundamental Solutions for the Impulse Responses Reconstruction in Arbitrarily Shaped Plates

Alexandre Leblanc, Antoine Lavie, Ros Ing

► To cite this version:

Alexandre Leblanc, Antoine Lavie, Ros Ing. The Method of Fundamental Solutions for the Impulse Responses Reconstruction in Arbitrarily Shaped Plates. *Acta Acustica united with Acustica*, 2011, 97, pp.919 - 925. 10.3813/aaa.918473 . hal-03617580

HAL Id: hal-03617580

<https://hal.science/hal-03617580>

Submitted on 23 Mar 2022

HAL is a multi-disciplinary open access archive for the deposit and dissemination of scientific research documents, whether they are published or not. The documents may come from teaching and research institutions in France or abroad, or from public or private research centers.

L'archive ouverte pluridisciplinaire **HAL**, est destinée au dépôt et à la diffusion de documents scientifiques de niveau recherche, publiés ou non, émanant des établissements d'enseignement et de recherche français ou étrangers, des laboratoires publics ou privés.

The Method of Fundamental Solutions for the Impulse Responses Reconstruction in Arbitrarily Shaped Plates

Alexandre Leblanc¹⁾, Antoine Lavie¹⁾, Ros Kiri Ing^{2)*}

¹⁾ Univ Lille Nord de France, 59000 Lille, France. UArtois, LGCgE, 62400 Béthune, France.
alexandre.leblanc@univ-artois.fr

²⁾ Institut Langevin, Laboratoire Ondes et Acoustique, ESPCI, 10 rue Vauquelin, 75231 Paris cedex 05, France

Summary

In the present paper, impulse responses of thin isotropic plates of arbitrary shape and linear boundary conditions are determined from a set of measurements enclosing the area of interest. The used approach derives from the Method of Fundamental Solutions considering virtual monopolar sources in order to reconstruct the free vibration of the plate. The originality of this work lies in the practical deployment of this method: the collocation points are set in the plate and not at its boundaries as usually employed in eigenanalysis context. Also, an alternative formulation is presented for which only the relative placements of the virtual sources and the collocation points are needed to determine the weighting coefficients, without knowing the shape of the plate and its boundary conditions. Several measurements with 3 kinds of plates have been achieved and the results highlight the remarkable robustness of the proposed formulations even for plate of complicated shape with various boundary conditions.

PACS no. 43.40.Dx, 43.40.Sk, 43.40.At

Introduction

With the wide range of application of structures of complex geometry, analysis of plate vibration is still of primary importance. Although various analytical and numerical methods are available in the literature [1], with explicit formulas for some particular problems [2], exact analysis are usually difficult when the plate shape or the boundary conditions are complex. A standard finite difference method can produce good results when dealing with a particular type of shapes, defined on rectangular grids, otherwise the finite element method or the boundary element method are more appropriate [3].

The plate problem was also considered using meshfree methods as Kang *et al.* [4] who proposed the non-dimensional dynamic influence function method, Chen *et al.* [5] with a method using a radial basis function or Alves *et al.* [6] who employed the Method of Fundamental Solutions (MFS) for the eigenanalysis of 2D plates.

In this paper, an alternative meshfree method based on the principle of the MFS is proposed, for the vibration analysis of arbitrarily shaped plates and various boundary conditions. The basic idea is to decompose the solutions of a partial differential equation into a linear combination of the fundamental solutions, represented by vir-

tual source points. Usually, the intensities of the sources are the unknown parameters [7]. This principle has been extensively used and is known under various denominations as the Wave Superposition Method (WSM) [8], the sources simulation method [9], the auxiliary [10] or equivalent [11] sources method. While different in theoretical aspects, all these formulations substitute a real radiating body by a set of elementary sources, thus the global field of interest can be approximated by the sum of the fields due to each source. One of the most advantageous feature of these meshfree methods is to have a computational cost lower than usual boundary or finite element methods. Thus, these methods constitute efficient and economical simulation techniques for practical applications like active control. As a setback to the simplicity of its underlying principle, the determination of the source strengths leads to numerical and analytic difficulties, extensively discussed over the past two decades [6, 12]. It's worth noting that if the sources are located on a continuous contour, and employed to solve the Helmholtz equation, the MFS is equivalent to the WSM.

Starting from the fundamental solution of the governing differential equation of the plate, with an implicit domain considered, a wave-type function that propagates omnidirectionally is considered. Physically, this Green's function represents the response at a point B to a unit excitation at A. It thus defines a 1D function, as the only independent variable is the distance between A and B. So, the main idea of the proposed method is to reconstruct the response

Received 29 March 2011,
accepted 30 July 2011.

* Also at Denis Diderot University (Paris 7)

at B from a set of virtual sources surrounding the plate. This method ensures the equivalence between the measured and the reconstructed impulse response between A and B. Indeed, the proposed method differs strongly from other MFS applications to plate vibration as the collocation points are located inside the real bounded plate and not at its boundaries. This configuration is of primarily importance since it allows to take into account any boundary conditions at plate edges implicitly with ease of application thanks to vibration measurements at any point of the plate.

In the following section the MFS formulations used in this paper is shown. This underscores the matrix system needed to obtain the weighting coefficients associated at virtual sources. Also in this section, a new scheme of the classical MFS is proposed for which only the relative placements of the virtual sources and the collocation points are needed in order to determine the weighting coefficients. Thus, the main process of the MFS which is the determination of these weighting coefficients is simplified as its only involves unbounded-medium Green's functions with no knowledge about the plate boundary conditions. The third section concerns the applications performed using these different formulations applied to three kind of plates with various boundary conditions.

1. MFS formulation

The equation for harmonic free flexural vibration of an uniform thin plate is written as [2]

$$\nabla^4 w(\mathbf{r}) - k^4 w(\mathbf{r}) = 0, \quad (1)$$

where $w(\mathbf{r})$ is the function of transverse deflection, $k^4 = \omega^2 \rho h / D$ with ρ the density, ω the angular frequency, h the thickness of the plate, and D the flexural rigidity.

The fundamental solution of the equation equation (1) is defined by

$$\nabla^4 G(\mathbf{r}_A|\mathbf{r}) - k^4 G(\mathbf{r}_A|\mathbf{r}) = -\delta(\mathbf{r}_A - \mathbf{r}), \quad (2)$$

where \mathbf{r} represents the coordinates of field point and \mathbf{r}_A the coordinates of source point. The solution of the equation (2) is the Green's function defined by [13]

$$G(\mathbf{r}_A|\mathbf{r}) = \frac{1}{8k^2} \left(iH_0^{(1)}(kr) - \frac{2}{\pi} K_0(kr) \right). \quad (3)$$

$H_0^{(1)}$ is the Hankel function of the first kind, K_0 the modified Bessel function of the second kind, $r = |\mathbf{r} - \mathbf{r}_A|$ the distance between the plate excitation placed at \mathbf{r}_A , and its measurement at \mathbf{r} .

In the MFS, the solution is assumed to be [14]

$$w(\mathbf{r}) \approx \sum_{j=1}^N \left\{ \alpha_j H_0^{(1)}(k|\mathbf{r} - \mathbf{s}_j|) + \beta_j K_0(k|\mathbf{r} - \mathbf{s}_j|) \right\}, \quad (4)$$

where α_j and β_j are the intensities of the virtual source point at \mathbf{s}_j , and N the number of virtual source points as depicted in Figure 1.

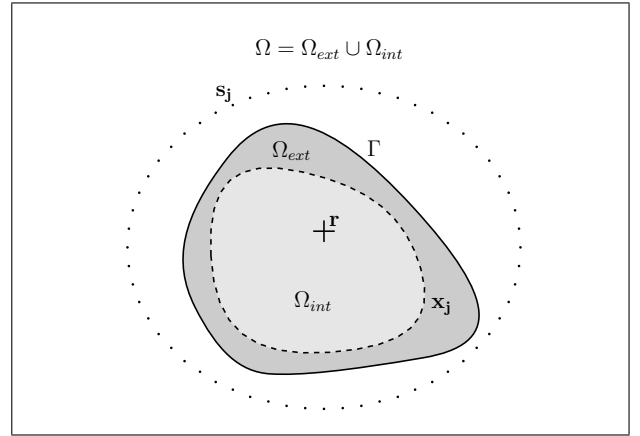


Figure 1. Geometry configuration of the MFS for plate vibrations.

Classically, in order to obtain the unknown intensities, boundary field points are chosen to satisfy the specified boundary conditions of the plate. Here, for practical reasons concerning measures and for some cases to quantify only propagative waves, collocation points are selected in Ω . In order to be able to reconstruct the area of interest Ω_{int} with minimal measurements, these collocation points should define a contour bounding Ω_{int} . One should notice that two weighting coefficients are associated for each virtual source locations, α for the propagative and β for the evanescent waves. Thus, for N virtual sources, $2N$ collocation points \mathbf{x}_j (where w is measured) are needed. From equation (4), this results in a $2N \times 2N$ linear system,

$$[A]_{2N \times 2N} \begin{bmatrix} [\alpha]_N \\ [\beta]_N \end{bmatrix} = [w(\mathbf{x})]_{2N}, \quad (5)$$

where $[A]$ represents the influence matrix between the virtual sources and the collocation points in terms of fundamental solutions,

$$[A] = \begin{bmatrix} H_0^{(1)}(k|\mathbf{x}_1 - \mathbf{s}_1|) & \cdots & K_0(k|\mathbf{x}_1 - \mathbf{s}_N|) \\ \vdots & \ddots & \vdots \\ H_0^{(1)}(k|\mathbf{x}_{2N} - \mathbf{s}_1|) & \cdots & K_0(k|\mathbf{x}_{2N} - \mathbf{s}_N|) \end{bmatrix}. \quad (6)$$

Then, determination of the unknown weighting coefficients is straightforward using matrix inversion.

This scheme is effective to handle practical applications as the boundary conditions are not needed to reconstruct plate vibrations but simply incorporated *via* the displacement measure at collocation points. Knowing the dispersive property of the medium, determination of the coefficients α_j and β_j leads to evaluate $w(\mathbf{r})$ anywhere in Ω_{int} thanks to equation (4):

$$w(\mathbf{r}) \approx \begin{bmatrix} [\alpha] \\ [\beta] \end{bmatrix}^T \begin{bmatrix} H_0^{(1)}(k|\mathbf{r} - \mathbf{s}|) \\ K_0(k|\mathbf{r} - \mathbf{s}|) \end{bmatrix}. \quad (7)$$

A simplification of the reconstruction system defined by equation (5) is also possible. In fact, evanescent waves can be generally neglected when dealing with plates of large

dimensions in respect to the investigated wavelengths. The resulting matrix system is therefore directly applicable to simply supported plates or fixed membranes where evanescent waves are not generated at plate boundaries. The first term of equation (3) corresponds to a propagating wave whereas the second term corresponds to an evanescent wave. In the proposed method, those waves can generally be ignored since we observe the plate only in its interior domain. Indeed, the evanescent waves decrease quickly, -20 dB per $\lambda/3$, compared to the propagating waves [15]. This assumption recovers the far-field Hankel approximation of the fundamental solution for the infinite plate [16, 17]. If neglecting the evanescent waves (thus solving a bidimensional Helmholtz equation [2]) and if the sources are distributed along a continuous contour as shown in Figure 1, an application of the WSM can also be performed [8]. For the MFS, and since equation (1) can be reduced to the membrane equation ($\nabla^2 w + k^2 w = 0$), the linear system defined in equation (4) is recast only for the weighting coefficients related to the propagative waves,

$$w(\mathbf{r}) \approx [\alpha]^T \left[H_0^{(1)}(k|\mathbf{r} - \mathbf{s}|) \right]. \quad (8)$$

The weighting coefficients α are obtained easily thanks to the collocation points,

$$\begin{bmatrix} \alpha_1 \\ \vdots \\ \alpha_N \end{bmatrix} = \begin{bmatrix} H_0^{(1)}(k|\mathbf{x}_1 - \mathbf{s}_1|) & \cdots & H_0^{(1)}(k|\mathbf{x}_1 - \mathbf{s}_N|) \\ \vdots & \ddots & \vdots \\ H_0^{(1)}(k|\mathbf{x}_N - \mathbf{s}_1|) & \cdots & H_0^{(1)}(k|\mathbf{x}_N - \mathbf{s}_N|) \end{bmatrix}^{-1} \cdot \begin{bmatrix} w(\mathbf{x}_1) \\ \vdots \\ w(\mathbf{x}_N) \end{bmatrix} = [A'] [w(\mathbf{x})]. \quad (9)$$

Thus, the reconstruction process consists of two main steps:

- compute the weighting coefficients α and β (resp. α) with measures at collocation points *via* equation (5) (respectively equation 9),
- associate these coefficients with free-space Green's function (cf. equation 7 or 8).

1.1. Alternative formulation

An alternative formulation for the weighting coefficients determination is possible. Expliciting the weighting coefficients in equation (7) with equation (5), we have

$$w(\mathbf{r}) \approx ([A]^{-1} [w(\mathbf{x})])^T \begin{bmatrix} H_0^{(1)}(k|\mathbf{r} - \mathbf{s}|) \\ [K_0(k|\mathbf{r} - \mathbf{s}|)] \end{bmatrix}. \quad (10)$$

This equation can be recast as

$$w(\mathbf{r}) \approx \left(([A]^T)^{-1} \begin{bmatrix} H_0^{(1)}(k|\mathbf{r} - \mathbf{s}|) \\ [K_0(k|\mathbf{r} - \mathbf{s}|)] \end{bmatrix} \right)^T [w(\mathbf{x})]. \quad (11)$$

This leads to another MFS formulation with new weighting coefficients $\tilde{\alpha}$ and $\tilde{\beta}$,

$$w(\mathbf{r}) \approx \begin{bmatrix} \tilde{\alpha} \\ \tilde{\beta} \end{bmatrix}^T [w(\mathbf{x})]. \quad (12)$$

Here these coefficients are computable without any prior measurements on boundary conditions as we have

$$\begin{bmatrix} \tilde{\alpha} \\ \tilde{\beta} \end{bmatrix} = ([A]^T)^{-1} \begin{bmatrix} H_0^{(1)}(k|\mathbf{r} - \mathbf{s}|) \\ [K_0(k|\mathbf{r} - \mathbf{s}|)] \end{bmatrix}. \quad (13)$$

Once again, if the evanescent waves can be neglected, equation (12) is simplified,

$$w(\mathbf{r}) \approx [\tilde{\alpha}]^T [w(\mathbf{x})]. \quad (14)$$

The weighting coefficients $\tilde{\alpha}$ are thus obtained by

$$[\tilde{\alpha}] = \left([A']^T \right)^{-1} \begin{bmatrix} H_0^{(1)}(k|\mathbf{r} - \mathbf{s}|) \end{bmatrix}. \quad (15)$$

Comparing this last equation with the classical MFS scheme defined by equation (8), the process is somehow reversed:

- compute the weighting coefficients $\tilde{\alpha}$ and $\tilde{\beta}$ (resp. $\tilde{\alpha}$) with free-space Green's function only *via* equation (13) (resp. (15)),
- associate these coefficients with measures at collocation points (cf. equation 12 or equation 14).

This procedure can be useful when dealing with plate of same dispersive properties but different shapes and various boundary conditions.

2. MFS Applications

The usual and alternative MFS formulations presented in this paper are investigated for three different plates:

- rectangular inox plate, clamped at one edge, free on the others. Equation (4) is employed here, because of significant evanescent waves in the reconstruction area.
- circular glass mirror with one segment cut off, with free edges. As only propagating waves are considered in the reconstruction area, equation (8) is used.
- complex-shaped inox plate, clamped at one edge, free on the others. Again, only propagating waves are expected in the area of interest, equation (14) is evaluated.

These three cases also highlight the potential of the proposed method for impulse responses reconstruction in arbitrarily shaped plates. Indeed, after a first case dealing with the space reconstruction of plate vibration at a discrete frequency, the frequency responses obtained by the MFS process can be treated by inverse discrete Fourier transform in order to obtain the corresponding impulse responses.

2.1. Numerical considerations

Matrix inversion: basic rank-revealing decompositions show the rank-deficient nature of numerical problems defined by methods based on fundamental solutions. For the following applications, truncated singular value decomposition [18] are performed to compute efficiently the weighting coefficients with the use of equations (5) or (9).

Fictitious eigenfrequencies: an issue of the MFS is the existence of the fictitious eigenfrequencies when the sources network defines a closed contour or surface. As

it has been proved for the WSM, these methods share the same uniqueness problem at characteristic frequencies.

Several solutions exist to circumvent this indetermination, one of the easiest to implement in the present case is to place few other collocation points out of the main collocation points network [19].

Number of collocation points: when the discrete set of the collocation points defines an outline, the accuracy of the MFS depends solely of the classic frequency criterion seen in previous works on the WSM, setting the maximum recommended distance between two points at $\lambda/3$ [20]. Increasing the collocation points density has shown no significant improvement on method accuracy. On the contrary, as the condition number of the influence matrix increases with the number of collocation points, this may have the opposite effect on the method reliability.

Acoustic dispersion: the dispersive relation, used in the following applications, between k and the frequency f is given by the low-frequency approximation $k^2 = 2\pi\sqrt{3}f/V_p h$ [21], where V_p is the plate velocity as defined in [22].

2.2. Experimental setup

Figure 2 shows the experimental setup deployed in order to acquire the normal displacements needed to validate the present method. The impulse responses are measured using glued PZT ceramic acting as an emitter, and a laser vibrometer acting as a receiver at the observation point in Ω_{int} and for the normal displacements measurement at collocation points. The diameter of the piezoelectric disk is 10 mm. The signal used to excite the PZT ceramic is a chirp signal of varying frequency (from 3 kHz to 20 kHz) and driven by a standard audio card with a 44 kHz sampling rate. This impulse load acting results in an initial velocity and the response due to such loading can be thought as free vibration under the initial velocity. For the 2nd application, for which the edges are supposed free, the plate is supported by 3 foam blocks. Comparisons with a plate for which a solution is known [2] have validated this setup.

2.3. Experimental results

The first experiment is performed on a rectangular inox plate (length $L_p = 190$ mm, width $W_p = 130$ mm, $h = 2$ mm and $V_p = 3725$ m/s). This plate is clamped at one of its widths and free to vibrate at the three other edges. Here, equation (5) is employed in order to determine the unknown intensities for both propagative and evanescent virtual sources. The collocation points define two outlines:

- the exterior outline defines the reconstruction area Ω_{int} ,
- the interior outline is use for numerical stability and could be placed anywhere in Ω_{int} .

Indeed, the few interior collocation points added to the exterior set of collocation points cancel the fictitious resonance frequencies of the rectangular contour. Without these additional measures, the correlation level will depend mainly on the fictitious resonances density, which can be irrelevant for small plate but cancel the efficiency

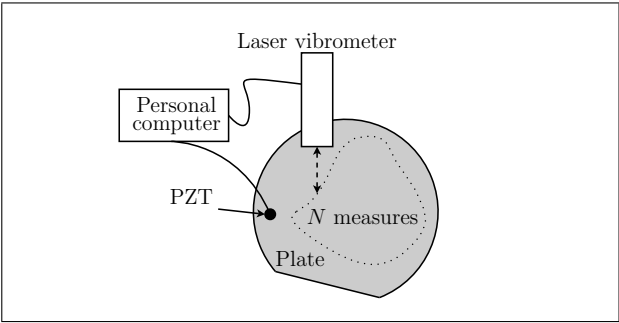


Figure 2. Experimental setup.

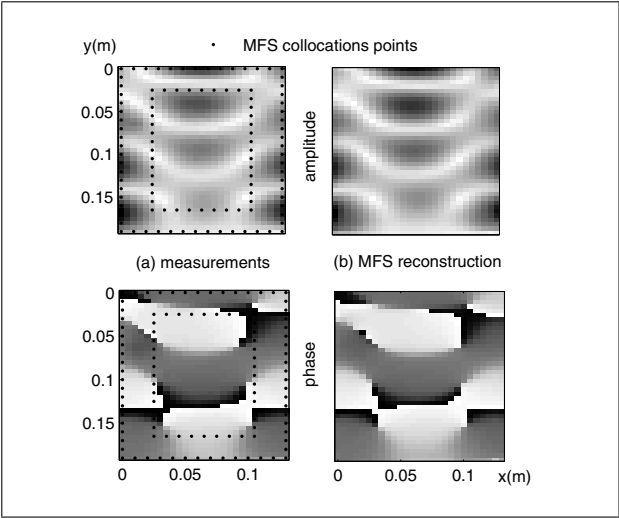


Figure 3. Measured and reconstructed amplitude and phase by the MFS algorithm ($N = 108$) at 3.4 kHz.

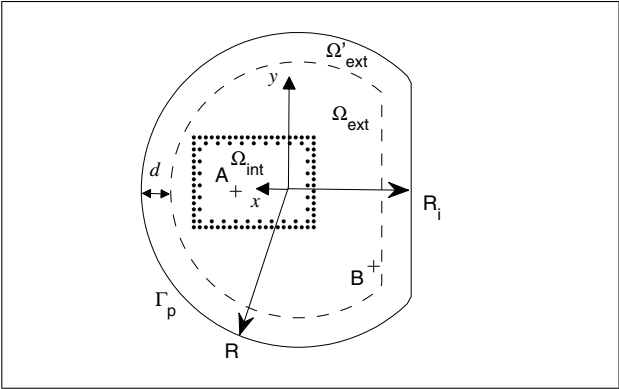


Figure 4. Truncated glass plate, •: collocation points ($N = 99$).

of the proposed method for common plate or high frequencies investigation. It must be remembered that these eigenfrequencies are only linked to the geometrical disposition of the collocation points and not to the real plate physical boundaries.

Figure 3 shows the reconstruction of the normal displacements in all the plate domain from these 108 collocation points and with a virtual sources outline set to be a homothetic transformation of ratio 2 of the exterior outline.

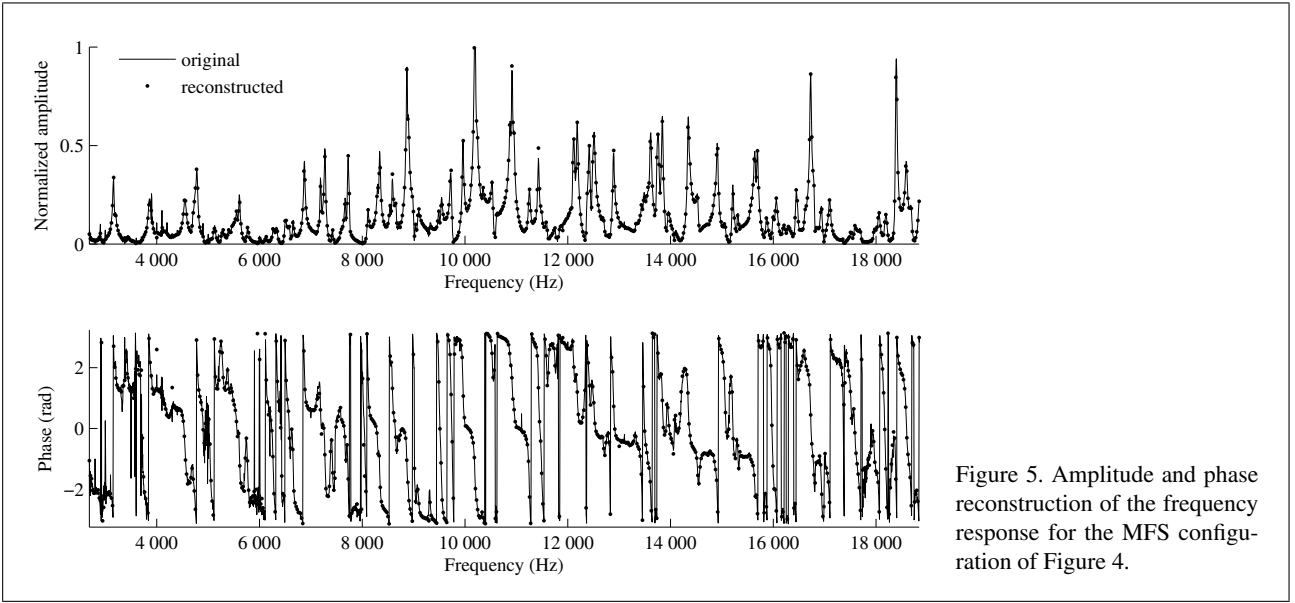


Figure 5. Amplitude and phase reconstruction of the frequency response for the MFS configuration of Figure 4.

The Mean Square Error (MSE) obtained by the method is less than 1.2% at collocation points and less than 5% for the whole plate surface. This estimator is defined as

$$\text{MSE} = \sqrt{\frac{\sum_{i=1}^N |w_c(f, \mathbf{x}_i) - w_m(f, \mathbf{x}_i)|^2}{\sum_{i=1}^N |w_m(f, \mathbf{x}_i)|^2}}, \quad (16)$$

where w_c (resp. w_m) is the calculated displacement (resp. measured) w at the measure points.

With equation (9), then neglecting the evanescent field reconstruction, the MFS leads to higher error value (MSE > 20%), as expected.

The second application is carried out on a circular glass mirror with one segment cut off (Figure 4, radius $R = 210$ mm, $h = 4$ mm, radius of cutting $R_i = 150$ mm and $V_p = 5315$ m/s). This plate is homogeneous with free edges. For this application, equations (8) and (9) are employed, thus the collocation points can not be placed anywhere: the distance d defines the area where the evanescent waves can not be ignored. The point A is surrounded by a rectangular collocation points network with again few additional interior points to cancel the fictitious resonance frequencies. With the low-frequency approximation on dispersion, $d \approx 37$ mm if the lowest frequency of interest is 3 kHz. The axes origin is the center of mass of the mirror. The MFS scheme is used for an observation point located at A ($x = -74$ mm and $y = -2$ mm) and a PZT ceramic glued at B ($x = 110$ mm and $y = -102$ mm). The virtual sources are located on a circle of radius $2R$ and centered on axes origin.

Figure 5 shows the amplitude and the phase reconstructed at A compared to the original measure. The measured frequency response can be quantitatively compared to that determined from the MFS using a correlation indicator defined

$$\text{corr}(x, y) = \frac{1}{p} \sum_{i=1}^p \text{Re} \left(\frac{w_c(f_i, \mathbf{x}_A) \cdot w_m(f_i, \mathbf{x}_A)^*}{|w_c(f_i, \mathbf{x}_A) \cdot w_m(f_i, \mathbf{x}_A)|} \right), \quad (17)$$

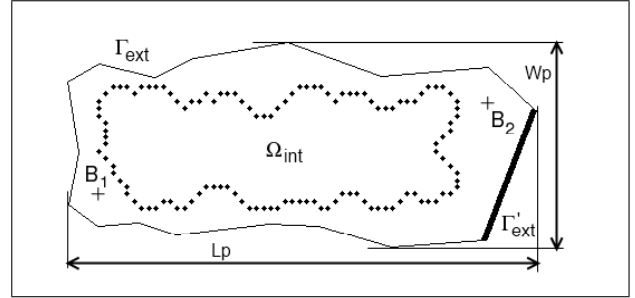


Figure 6. Polygonal plate, •: collocation points ($N = 121$).

where p denote the number of discrete frequencies for which the MFS is performed. Here, high level of correlation is achieved (up to 98% for this example).

The last application consists in the structural vibration reconstruction of an arbitrarily shaped inox plate (cf. Figure 6). The plate characteristics dimensions are $L_p = 355$ mm, $W_p = 130$ mm and $h = 2$ mm. Plate velocity is estimated at 4640 m/s.

Here, the plate is clamped at Γ'_{ext} with free edges for Γ_{ext} . Two chirp signals are alternately emitted from the two PZT ceramics at B_1 and B_2 and the displacement induced at original source location is measured by the laser vibrometer. equation (14) is used here in order to demonstrated the robustness of the alternative MFS formulation when dealing with a plate of complex shape and boundary conditions.

Figure 7 illustrates the reconstruction quality with correlation map for more than 600 locations of observation points A in Ω_{int} and for 121 sources disposed on a circular contour (radius = L_p) exterior to Γ_{ext} and Γ'_{ext} and centered at the center of mass. For the working band frequency from 3 kHz to 20 kHz, the results are particularly good as the reconstructed displacement is close to the collocation points. Nevertheless, correlation levels for the in-

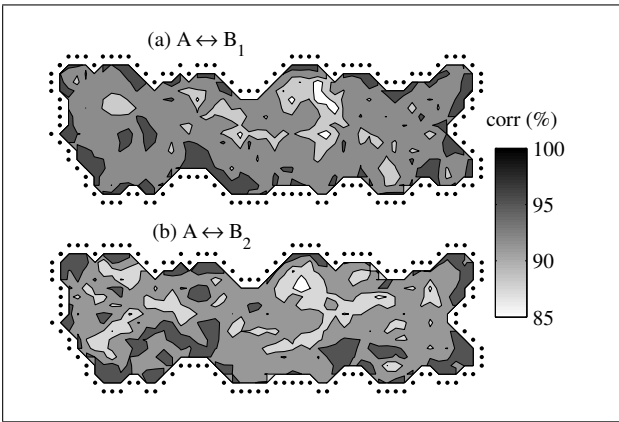


Figure 7. Polygonal plate: correlation maps for the reconstruction of the impulse response measured at $A \in \Omega_{int}$: (a) from B_1 - (b) from B_2 (cf. Figure 6)

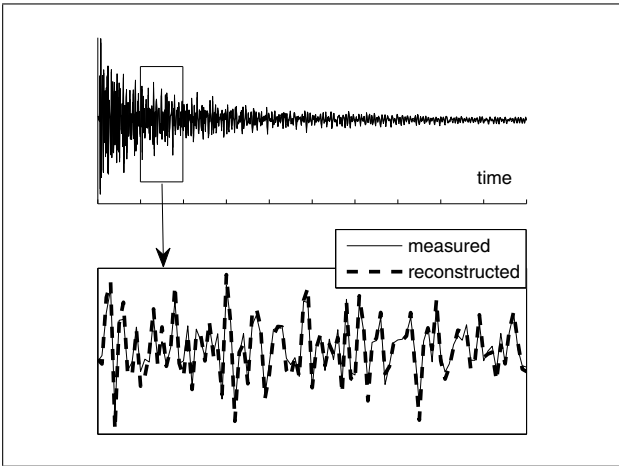


Figure 8. Polygonal plate: impulse response reconstruction example.

ner area are largely satisfactory with a mean value of 0.93 and a standard deviation of 0.02.

Finally, and to demonstrate the ability of the proposed formulation for the determination of the impulse response, the same plate is used but with an excitation signal now from 500 Hz to 20 kHz. Thus, prior considerations on the evanescent waves should be invalidated by the added low frequency band. Nevertheless, and as illustrated by Figure 8 for a point near the center of mass, results show remarkable agreement between the measured and reconstructed impulse response obtained via inverse discrete Fourier transform.

The robustness of the proposed method can be explained by the fact that most of the mechanical energy stands in the 3 kHz - 20 kHz range as shown in Figure 9.

3. Conclusion

Compared to usual techniques applied to the determination of the plate impulse responses, the MFS presents a real benefit in terms of measurement needs. With minimal material properties or boundary conditions knowledge, only a

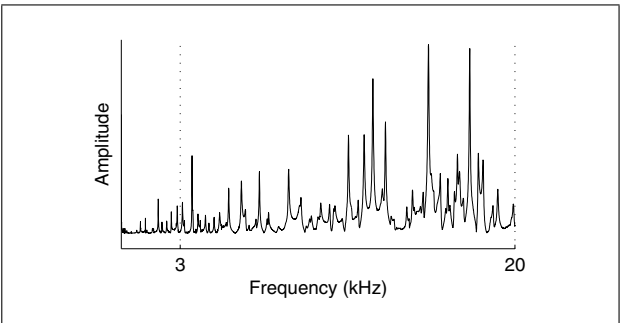


Figure 9. Polygonal plate: frequency response for the measured point of Figure 8.

contour discretization inside the plate is required to compute efficiently the transverse displacements with no assumptions on geometry. Excellent results are obtained for both rectangular and complex-shaped thin plates, showing the quality and the robustness of the proposed method. When the evanescent waves are taken into account, the method could be also applied to plate with arbitrary holes or cutouts. Further developments and experiments should be carried out to establish the limits of this approach.

References

[1] K. F. Graff: Wave motion in elastic solids. Dover, New York, 1991.

[2] A. W. Leissa: Vibration of plates. Acoustical Society of America, New York, 1993.

[3] G. D. Manolis, D. E. Beskos: Boundary element methods in elastodynamics. Taylor & Francis, London, 1998.

[4] S. W. Kang, J. M. Lee: Free vibration analysis of arbitrary shaped plates with clamped edges using wave-type functions. *J. Sound Vibr.* **242** (2001) 9–16.

[5] J. T. Chen, I. L. Chen, K. H. Chen, Y. T. Lee, Y. T. Yeh: A meshless method for free vibration analysis of circular and rectangular clamped plates using radial basis function. *Eng. Anal. Boundary Elem.* **28** (2004) 535–545.

[6] C. J. S. Alves, P. R. S. Antunes: The method of fundamental solutions applied to the calculation of eigensolutions for 2d plates. *Int. J. Numer. Meth. Engng.* **77** (2009) 177–194.

[7] G. Fairweather, A. Karageorghis, P. A. Martin: The method of fundamental solutions for scattering and radiation problems. *Eng. Anal. Boundary Elem.* **27** (2003) 759–769.

[8] G. H. Koopmann, L. Song, J. B. Fahnlne: A method for computing acoustic fields based on the principle of wave superposition. *J. Acoust. Soc. Am.* **86** (1989) 2433–2438.

[9] R. Kress, A. Moshen, B. Brosowski: On the simulation source technique for exterior problems in acoustics. *Math. Methods Appl. Sci.* **8** (1986) 585–597.

[10] S. A. Yang: A boundary integral equation method using auxiliary interior surface approach for acoustic radiation and scattering in two dimensions. *J. Acoust. Soc. Am.* **112** (2002) 1307–1317.

[11] M. E. Johnson, S. J. Elliott, K.-H. Baek, J. Garcia-Bonito: An equivalent source technique for calculating the sound field inside an enclosure containing scattering objects. *J. Acoust. Soc. Am.* **104** (1998) 1221–1231.

[12] D. T. Wilton, I. C. Mathews, R. A. Jeans: A clarification of nonexistence problems with the superposition method. *J. Acoust. Soc. Am.* **94** (1993) 1676–1680.

- [13] J. Vivoli, P. Filippi: Eigenfrequencies of thin plates and layer potentials. *J. Acoust. Soc. Am.* **55** (1974) 562–567.
- [14] D. Young, C. Tsai, Y. Lin, C. Chen: The method of fundamental solutions for eigenfrequencies of plate vibrations. *Computers, Materials & Continua* **4** (2006) 1–10.
- [15] G. Ribay, D. Clorennec, S. Catheline, M. Fink, R. Ing, N. Quieffin: Tactile time reversal interactivity: Experiment and modelization. 2005 IEEE Ultrasonics Symposium, Vols. 1–4, 2005, 2104–2107.
- [16] R. Gunda, S. M. Vijayakar, R. Singh, J. E. Farstad: Harmonic Green's functions of a semi-infinite plate with clamped or free edges. *J. Acoust. Soc. Am.* **103** (1997) 888–899.
- [17] N. N. Lebedev: Special functions and their applications. Dover, New-York, 1972.
- [18] C. Hansen: The truncated SVD as a method for regularization. *BIT* **27** (1987) 534–553.
- [19] A. Leblanc, R. K. Ing, A. Lavie: A wave superposition method based on monopole sources with unique solution for all wave numbers. *Acta Acustica united with Acustica* **96** (2010) 125–130.
- [20] L. Song, G. H. Koopmann, J. B. Fahline: Numerical errors associated with the method of superposition for computing acoustic fields. *J. Acoust. Soc. Am.* **89** (1991) 2625–2633.
- [21] N. Etaix, A. Leblanc, M. Fink, R.-K. Ing: Thickness or phase velocity measurements using the Green's function comparison method. *IEEE Trans. Ultrason. Ferroelectr. Freq. Control.* **57** (2010) 1804–1812.
- [22] D. Royer, E. Dieulesaint: Elastic waves in solids 1. Springer, Berlin, 1996.